Ecological Modelling 468 (2022) 109909

Contents lists available at ScienceDirect

Ecological Modelling

journal homepage: www.elsevier.com/locate/ecolmodel

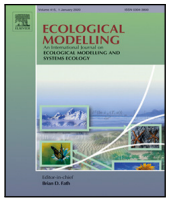

Kinetics of phosphate uptake in the dinoflagellate *Karenia mikimotoi* in response to phosphate stress and temperature

Shufei Gao [a,1], Anglu Shen [b,1], Jie Jiang [a,1], Hao Wang [c], Sanling Yuan [a,*]

[a] College of Science, Research Center of Mathematical Biology and Big Data, University of Shanghai for Science and Technology, Shanghai 200093, China
[b] College of Marine Ecology and Environment, Shanghai Ocean University, Shanghai 201306, China
[c] Department of Mathematical and Statistical Sciences, University of Alberta, Edmonton, Alberta T6G 2G1, Canada

ARTICLE INFO

Keywords:
Algal bloom
Competition
Prorocentrum donghaiense
Surface adsorption
Two-stage model

ABSTRACT

Phosphate (P_i) and temperature are two important environmental factors affecting algal growth and the occurrence of red tide. In this paper, we conduct experiments on *Karenia mikimotoi* under different P_i concentrations and temperatures and propose a novel P_i uptake model by incorporating Arrhenius function and P_i-stress function into the two-stage model presented in one of our recent paper (Jiang et al. (2019)). In both P_i-replete and P_i-deplete, the model parameters are obtained by fitting the experimental data at 24 °C and validated by the experimental data at 20 °C, respectively. *K. mikimotoi* under low P_i condition entered into the exponential growth phase earlier compared with P_i-replete groups. Under the P_i-replete condition, *K. mikimotoi* continually increased, while the P_i-deplete condition showed a wave trend. The experimental results and the fitting of experimental data both show that *K. mikimotoi* has an obvious response to temperature. In both P_i-replete and P_i-deplete, the peak values of the cell quota of intracellular P_i and surface-adsorbed P_i at 24 °C were higher than those at 20 °C. Using the luxury coefficient and growth potential, interspecific competition between *K. mikimotoi* and *Prorocentrum donghaiense* is also discussed. These results and conclusions are helpful to understand the P_i uptake characteristics of algae at different P_i concentrations and temperatures, and could effectively explain mechanisms of interspecific competition and succession between different algae species during red tide.

1. Introduction

Karenia mikimotoi (formerly named *Gymnodinium mikimotoi* Brand et al., 2012), a widely distributed red tide species, is known to form alternating blooms with some other harmful algae species (e.g., *Prorocentrum donghaiense*, *Heterocapsa circularisquama* and so on) (Chang, 2011; Li et al., 2009; Uchida et al., 1999). Since 1998, the blooms of *K. mikimotoi* have often been seen in the coastal waters of the Zhejiang and Fujian provinces in China and have caused heavy losses in aquaculture and deterioration of the marine ecological environment (Zhao, 2010; Li et al., 2019; Lü et al., 2019). It is found that after diatom blooms, the concentration of phosphate (P_i) is relatively low in the coastal water of the East China Sea (Li et al., 2009; Zhao, 2010), and the previous studies showed that the P_i uptake rate in cells with P_i-stress is higher than that without P_i-stress (Lehman and Sandgren, 1982; Riegman and Mur, 1984; Lin et al., 2016). On the other hand, the temperature is also a major factor controlling photosynthesis which has a close relationship with the metabolism and growth of algae (Helbling et al., 2011; Shen et al., 2016; Davison, 1991). It can affect the maximum growth rate of algae (Goldman and Carpenter, 1974), thereby changing the P_i uptake rate of algae cells and affecting the alternations of algal blooms (Karentz and Smayda, 1984). During most *K. mikimotoi* blooms, the sea surface temperature ranges from 18 °C to 26 °C (Zhao, 2010; Chen et al., 2003; Zhou et al., 2017b,a). The highest specific growth rate of *K. mikimotoi* is obtained at 24 °C (Shen et al., 2016), and the average sea surface temperature from 2001 to 2010 was 23.6 °C when blooms of *K. mikimotoi* occurred in the East China Sea (Zhao, 2010). Hence, it is important to understand the kinetics of P_i uptake by algae under different conditions of P_i concentration and temperature.

In many previous studies, the Michaelis–Menten equation has often been used to describe the nutrient uptake process by algae (Lee et al., 2015). However, the successful use of Michaelis–Menten kinetics model to describe nutrient uptake often masks the difficulties in interpreting the kinetics parameters obtained by measurement (Droop, 1983). In addition, the two-parameter Michaelis–Menten kinetics model cannot

* Corresponding author.
E-mail address: sanling@usst.edu.cn (S. Yuan).
[1] The contribution of the authors to the study is equal and shall be considered as co-first author.

https://doi.org/10.1016/j.ecolmodel.2022.109909
Received 28 June 2020; Received in revised form 5 February 2022; Accepted 10 February 2022
Available online 12 March 2022
0304-3800/© 2022 Elsevier B.V. All rights reserved.

well describe the observed phenomenon of "luxury uptake" of algae cells under P_i-stress (Goldman et al., 1981; Harrison et al., 1976, 1989). Therefore, it is not enough to describe the P_i uptake process of microalgae only by Michaelis–Menten kinetics. Within the adaptive range, algae can maintain the maximum growth rate by adjusting their internal nutrient quota and absorbing nutrients at the maximum short-term nutrient uptake rate according to changes in external nutrient concentration (Morel, 1987). Aksnes and Egge (1991) developed a phytoplankton nutrient uptake rate model described by $V = nAvS/(1 + hAvS)$, where V is the uptake rate, n is the number of cellular uptake sites, A is the area of uptake sites, h is the time required for processing one nutrient ion, v is the mass transfer coefficient, S is the nutrient concentration in the substrate, and confirmed that the Michaelis–Menten equation applied to the uptake process of algae was a special case of the model. In fact, this model can be rearranged as $V = nh^{-1}S/((hAv)^{-1} + S)$, which can then be transmitted to the classical Michaelis–Menten kinetics model by letting $V_{\max} = nh^{-1}$ and $K_S = (hAv)^{-1}$. Harrison et al. (1989) suggested that the maximum uptake rate of cells should be related to the size of the intracellular P_i pools. Considering the multiple P_i pools in cells, John and Flynn (2000) established the three-compartment P_i model of microalgal growth (phosphate interaction model, PIM). Recently, Singh et al. (2018) further extended the PIM model by considering the combined effects of light and nutrients on algal growth.

Notice that most studies mentioned above only considered the transportation from substrate into cells. In fact, the intracellular P_i (QP) pool and surface-adsorbed P_i (AP) pool have great significance to the investigation of P_i uptake kinetics of phytoplankton (Harrison et al., 1989; Jiang et al., 2019; Yao et al., 2011; Sañudo-Wilhelmy et al., 2004; Jin et al., 2021). The coexistence of QP pool and AP pool demonstrate that the P_i uptake process of algae should be divided into two stages: substrate P_i (WP) is first adsorbed on the cell surface and then AP enters the interior of cell to become QP through the active transport of membrane. Considering the effects of AP and QP on algal growth, Liu et al. (2007) established a two-stage growth kinetics model of algae. By further considering the regulation via transport-inhibition from size of QP pool, Yao et al. (2011) constructed a two-stage kinetics model of P_i uptake by algae based on the experimental data of short-term absorption kinetics of a green algae *Scenedesmus quadricauda*. Based on the phosphate absorption experimental data of *Prorocentrum donghaiense* under different phosphorus concentrations, in a recent paper (Jiang et al., 2019), we proposed a two-stage P_i uptake kinetics model with the Droop equation describing the dependence of cell growth on the QP based on the model of Yao et al. (2011). In Refs. Jiang et al. (2019) and Yao et al. (2011), the two-stage model and the traditional one-stage model were compared. From the model fitting results, the biological significance of parameters, and statistical test results et al. the two-stage model provides a more reasonable and realistic explanation for the process of P_i uptake by algae.

To better understand the effects of different P_i concentrations and temperatures on the P_i uptake kinetics of algae, in the present paper, the temperature function (Arrhenius function) and P_i stress function are further introduced to the model given in Jiang et al. (2019) and obtain a novel two-stage kinetics model. The parameter calibration and validation of the model are carried out based on the experimental data of P_i uptake by *K. mikimotoi* under different P_i concentrations and temperatures. Then, the effects of P_i concentration and temperature on P_i uptake characteristics of *K. mikimotoi* are analyzed by experimental data and parameter fitting results. The impact of different P_i uptake characteristics of *P. donghaiense* and *K. mikimotoi* on interspecific competition between these two species under different P_i concentrations and temperatures are also discussed.

2. Materials and methods

2.1. Model description

The process of P_i uptake by algae is divided into two steps. In the first step, P_i in the substrate is adsorbed to the cell surface. In the second step, P_i adsorbed on the cell surface is transported into the cell (see Jiang et al. (2019) for more details). We improve the model provided in Jiang et al. (2019) from the following two aspects.

Firstly, to clearly consider the influence of temperature on the growth rate of algae, the Arrhenius function is introduced into the model. The early P_i uptake model proposed by Droop (1973) presents a simple quota model in which the specific growth rate of algae (μ) is assumed to be a function of intracellular P_i concentration:

$$\mu = \mu_{\max} \cdot \frac{Q_c - Q_{\min}}{Q_c}, \tag{1}$$

where $\mu_{\max}$ is the maximum growth rate of algae, Q_c (10^{-8} μmol cell^{-1}) is the cell quota of QP (i.e., $Q_c = \mathrm{QP}/N$, where N is the cell density of algae) and $Q_{\min}$ is the minimum of Q_c. The maximum specific growth rate of algae, though independent of limiting nutrient concentrations, is still a function of other environmental variables such as temperature. Using the Arrhenius equation, $\mu_{\max}$ can be described as a function of temperature below (Goldman and Carpenter, 1974; Bordel et al., 2009):

$$\mu_{\max} = A \cdot \exp\left(-\frac{E}{K_b \cdot T}\right), \tag{2}$$

where T stands for the temperature, and the parameters A, E, K_b are respectively the maximum growth rate of algae at a particular temperature, activation energy for algal growth and universal gas constant. By substituting (2) into (1), then the specific growth rate of algae can be written as:

$$\mu = A \cdot \exp\left(-\frac{E}{K_b \cdot T}\right) \cdot \frac{Q_c - Q_{\min}}{Q_c}. \tag{3}$$

Secondly, to consider the influence of different P_i concentrations on the uptake kinetics of P_i by algae, the P_i stress function is introduced into the model. In the model of Jiang et al. (2019), the traditional Michaelis–Menten equation for P_i transport rate (PT) was modified as

$$\mathrm{PT} = K_p \cdot Q_{\max} \cdot \mu_{\max} \cdot \frac{S_p}{S_p + K_t} \cdot \frac{\left(1 - \frac{Q_c}{Q_{\max}}\right)^4}{\left(1 - \frac{Q_c}{Q_{\max}}\right)^4 + K_q}, \tag{4}$$

where K_p is a dimensionless coefficient describing P_i stress, $Q_{\max}$ is the maximum quota of P_i in the cell, and $K_p \cdot Q_{\max} \cdot \mu_{\max}$ represents the maximum transport rate (Yao et al., 2011); S_p (10^{-8} μmol cell^{-1}) is the cell quota of AP (i.e., $S_p = \mathrm{AP}/N$), K_t is the half-saturation constant from algal P_i uptake; and

$$\frac{\left(1 - \frac{Q_c}{Q_{\max}}\right)^4}{\left(1 - \frac{Q_c}{Q_{\max}}\right)^4 + K_q} \tag{5}$$

is a feedback function describing the regulation of the transport rate of P_i for each algal cell via the inhibition from the size of intracellular P_i pool, where K_q is a coefficient in the feedback control function. Notice that K_p describes the change of P_i uptake rate of algae under P_i stress, and there are literatures demonstrating that it is inversely proportional to phosphorus concentration in the environment (Dyhrman and Palenik, 1999; Rengefors et al., 2003; Yao et al., 2011). Algal cells can increase alkaline phosphatase activity and the number of high-affinity phosphate transporters under low phosphorus conditions to improve P_i uptake and utilization efficiency (Ou et al., 2008; Lin et al., 2016). To describe the P_i uptake characteristics of algae under different P_i concentrations, we propose the following P_i-stress function:

$$K_p = 1 + \frac{1}{\alpha \cdot \mathrm{WP} + \beta}, \tag{6}$$

Table 1
State variables of the two-stage model.

Variable	Unit	Explanation
WP	μM	P_i concentration in substrate
AP	μM	P_i concentration adsorbed on the cell surface
QP	μM	P_i concentration in the interior of the cell
N	$10^8\ cells\ L^{-1}$	Cell density of algae

where WP is the P_i concentration in substrate, and the parameters α and β are respectively the coefficient of WP affecting transport rate and a dimensionless coefficient in P_i-Stress function. Thus the final form of P_i transport rate can be represented as:

$$\mathrm{PT} = Q_{\max}\cdot\left(1+\frac{1}{\alpha\cdot\mathrm{WP}+\beta}\right)\cdot A\cdot\exp\left(-\frac{E}{K_b\cdot T}\right)\cdot\frac{S_p}{S_p+K_t}\cdot\frac{\left(1-\frac{Q_c}{Q_{\max}}\right)^4}{\left(1-\frac{Q_c}{Q_{\max}}\right)^4+K_q}. \tag{7}$$

Based on above, we can write out our novel P_i uptake kinetics model as follows:

$$\begin{cases}
\dfrac{\mathrm{d}N}{\mathrm{d}t} = \underbrace{\underbrace{\underbrace{A\cdot\exp\left(-\frac{E}{K_b\cdot T}\right)}_{\mu_{\max}:\ \text{Arrhenius equation}}\cdot\frac{Q_c-Q_{\min}}{Q_c}}_{\mu:\ \text{Droop equation}}\cdot N}_{\text{R: cell growth}} - \underbrace{e\cdot N}_{\text{D: cell death}},\\
\dfrac{\mathrm{dAP}}{\mathrm{d}t} = \underbrace{K_a\cdot\mathrm{WP}\cdot\left(1-\frac{S_p}{S_{p\max}}\right)}_{R_a:\ \text{absorption from substrate}} - \underbrace{K_d\cdot\mathrm{AP}}_{R_d:\ \text{desorption}}\\
\qquad - \underbrace{Q_{\max}\cdot\underbrace{\left(1+\frac{1}{\alpha\cdot\mathrm{WP}+\beta}\right)}_{K_p:\ P_i\text{-stress function}}\cdot A\cdot\exp\left(-\frac{E}{K_b\cdot T}\right)\cdot\frac{S_p}{S_p+K_t}\cdot\underbrace{\frac{\left(1-\frac{Q_c}{Q_{\max}}\right)^4}{\left(1-\frac{Q_c}{Q_{\max}}\right)^4+K_q}}_{F_q:\ \text{feedback function}}\cdot N}_{\text{PT: } P_i \text{ transport rate}},\\
\dfrac{\mathrm{dQP}}{\mathrm{d}t} = Q_{\max}\cdot\left(1+\frac{1}{\alpha\cdot\mathrm{WP}+\beta}\right)\cdot A\cdot\exp\left(-\frac{E}{K_b\cdot T}\right)\cdot\frac{S_p}{S_p+K_t}\cdot\frac{\left(1-\frac{Q_c}{Q_{\max}}\right)^4}{\left(1-\frac{Q_c}{Q_{\max}}\right)^4+K_q}\cdot N\\
\qquad - \underbrace{A\cdot\exp\left(-\frac{E}{K_b\cdot T}\right)\cdot\frac{Q_c-Q_{\min}}{Q_c}\cdot\mathrm{QP}}_{\text{dQP: dilution due to growth and birth}},\\
\dfrac{\mathrm{dWP}}{\mathrm{d}t} = -K_a\cdot\mathrm{WP}\cdot\left(1-\frac{S_p}{S_{p\max}}\right)+K_d\cdot\mathrm{AP},
\end{cases} \tag{8}$$

where $Q_c = \mathrm{QP}/N$ and $S_p = \mathrm{AP}/N$, other variables and parameters are provided respectively in Tables 1 and 2. Fig. 1 shows the conceptual diagram of model (8). The first equation of N in model (8) describes the cell growth with respect to QP quota. The second and the fourth equations describe respectively the P_i adsorption and desorption between cell surface and substrate. While the third equation describes the intracellular transportation of AP.

2.2. Experimental materials and methods

2.2.1. Algal culture conditions

Karenia mikimotoi was provided by Prof. Zhaoli Xu from East China Sea Fisheries Research Institute, Shanghai, China. The algae was pre-cultured at 20 °C in f/2 medium (Guillard, 1975) with a light intensity of 65–70 μmol photons m^{-2} s^{-1} cool-white light (12 : 12 h Light : Dark cycle, the photoperiod is from 6 AM to 6 PM). These cultures were manually shaken twice daily at 7:00 AM and 6:00 PM. These algal cells in the exponential growth phase were used in the following experiments.

Table 2
Parameters in the two-stage model.

Parameter	Unit	Explanation
K_q		Coefficient in the feedback control function
K_t	10^{-8} μmol $cell^{-1}$	Half-saturation constant from algal P_i uptake
$S_{p\max}$	10^{-8} μmol $cell^{-1}$	Maximum quota of surface adsorbed phosphate
$Q_{\max}$	10^{-8} μmol $cell^{-1}$	Maximum quota of phosphate in the cell
$Q_{\min}$	10^{-8} μmol $cell^{-1}$	Minimum quota of phosphate in the cell
K_a	day^{-1}	Adsorption rate
K_d	day^{-1}	Desorption rate
e	day^{-1}	Death rate
A	day^{-1}	Maximum growth rate of algae at a particular temperature
E	J mol^{-1}	Activation energy for algal growth
T	K	Absolute temperature
K_b	J $(mol\ K)^{-1}$	Universal gas constant
α	$(\mu M)^{-1}$	Coefficient of WP affecting transport rate
β		Dimensionless coefficients in P_i-Stress function

2.2.2. Temperature treatment experiments

To compare the growth rules of *K. mikimotoi* at different temperatures, these algal cells were cultured in 50 ml of fresh f/2 media in 100 ml Erlenmeyer flasks at an initial cell density of 0.2×10^8 cells L^{-1}. The temperatures of the flasks were set at 20 °C and 24 °C and the illumination condition as preculture.

2.2.3. Phosphate uptake experiments

The cell density of the algal cultures were about 0.2×10^8 cells L^{-1}, and the experiments were divided into P_i-replete group (25.55 μM P_i) and P_i-deplete group (0.74 μM P_i) with three replicates. A 10 mL sample was collected at the interval of 3 days in each group. The determination methods of WP, AP, and QP are based on Yao et al. (2011) and Jiang et al. (2019) with minor modifications. The cell density (N) was counted using the method of Jiang et al. (2019) at 0, 3, 6, 9, 12, 15, and 18 day.

2.2.4. Model calibration and validation

In this study, parameter values of model (8) are calibrated based on the experimental data (N, WP, Q_c, S_p) of *K. mikimotoi* at 24 °C under the conditions of P_i-replete and P_i-deplete by using the least square method, which is implemented by the function of "fmincon" of MATLAB R2016b. The least square estimation method is to find a set of optimal parameter values in parameter space to minimize the objective function. To get the objective function, the following model cost is used in this study (Adhurya et al., 2021):

$$cost_i = \sum_{j=1}^{n}\frac{(X_{ij}^{sim}-X_{ij}^{obs})^2}{X_{ij}^{obs^2}},$$

where $cost_i$ is the model cost of the ith state variable in parameter calibration, n is the number of observed data, X_{ij}^{sim} is the simulation value of the jth day of the ith state variable and X_{ij}^{obs} is the corresponding observed value of the jth day of the ith state variable. Model calibration of multiple variables simultaneously using the average cost of multiple variables as the objective function:

$$f(\Theta,m) = \frac{1}{m}\sum_{i=1}^{m}cost_i,$$

where Θ is a parameter vector to be calibrated, m is the number of state variables chosen to calibrate simultaneously.

After model calibration, experimental data (N, WP, Q_c, S_p) of *K. mikimotoi* at 20 °C under two P_i concentrations were used for model validation. In addition, the relative error is also calculated as another index to measure model fitness. The relative error between the simulation data and the observation data is calculated by the method

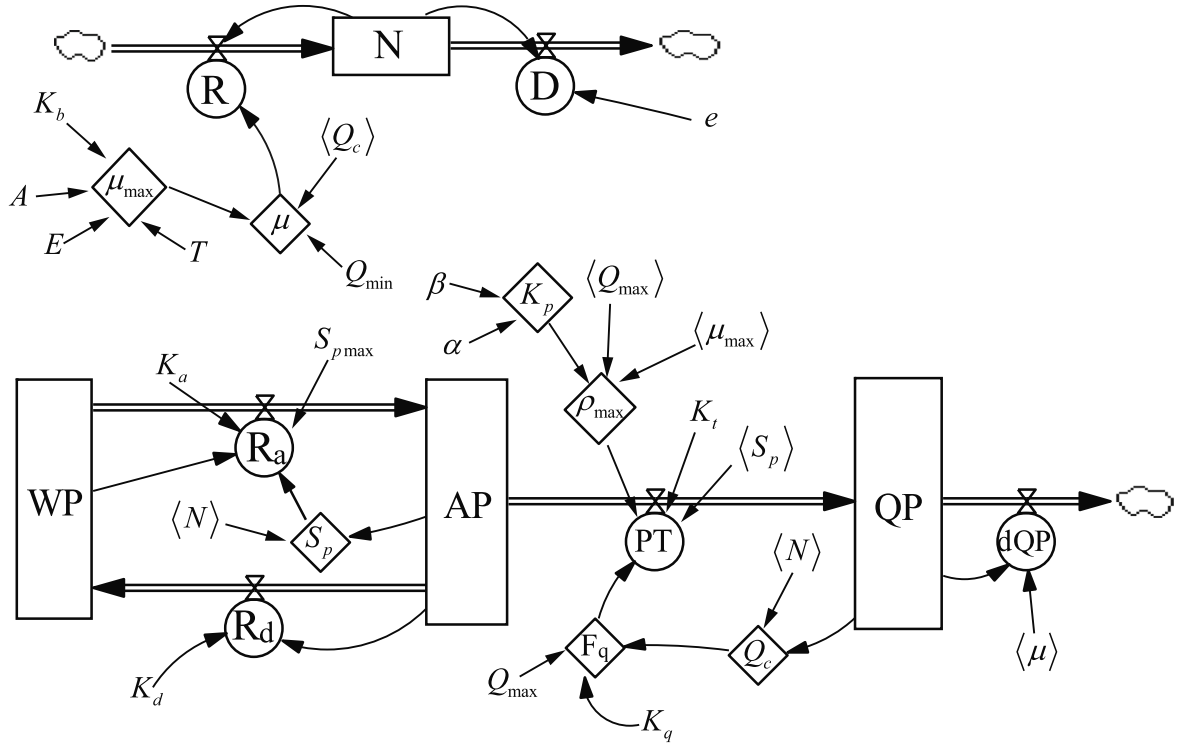

Fig. 1. The conceptual diagram of the two-stage model. Boxes are levels, circles are rates, diamonds are auxiliaries, square brackets are shadow variables, clouds represent sources or sinks, and the others are constants.

of Marois and Mitsch (2016),

$$RE_j = \left(\frac{X_j^{sim}}{X_j^{obs}} - 1 \right) \times 100,$$

where RE_j is the relative error, X_j^{sim} and X_j^{obs} are the simulation data and the observation data at jth day, respectively. The relative error of a state variable is expressed by the average relative error of all experimental data.

3. Results

3.1. Experimental results

3.1.1. Results of short-term phosphate absorption experiments of K. mikimotoi under P_i-replete condition

The changes of state variables N, WP, Q_c (cell quota of QP), and S_p (cell quota of AP) of *K. mikimotoi* at 20 °C and 24 °C under the condition of P_i-replete over time are shown in Fig. 2. With the initial cell density of 0.2×10^8 cells L^{-1}, N increased slowly during the early 6 days and increased quickly in the latter 12 days. When the initial P_i concentration in the substrate was 25.55 μM, the trends of WP in both 20 °C and 24 °C conditions ultimately reached a plateau after a sharp initial decline. WP at 24 °C decreased more significantly than WP at 20 °C. With the initial Q_c 6.70×10^{-8} μmol $cell^{-1}$, the trends of Q_c at 20 °C and 24 °C were identified as increasing in the early 3 or 6 days then decreasing. However, the maximum value of Q_c (16.33×10^{-8} μmol $cell^{-1}$) at 24 °C was larger than that at 20 °C (11.24×10^{-8} μmol $cell^{-1}$). With the initial S_p 19.68×10^{-8} μmol $cell^{-1}$, S_p at two temperatures increased in the first 3 days and dropped rapidly for the next 9 days then it maintained a more or less stable condition. The peak value of S_p at 24 °C was higher than that at 20 °C. In addition, the decline rates of S_p at the two temperatures were different from day 3 to day 12. At 24 °C, S_p first decreased slowly, then decreased rapidly, and finally decreased slowly, while at 20 °C, S_p declined almost linearly.

Table 3
Parameter values of model (8) are calibrated from experimental data of *K. mikimotoi* under P_i-replete and P_i-deplete condition at 24 °C.

Parameter	P_i-replete	P_i-deplete	Parameter	P_i-replete	P_i-deplete
K_q	0.0359	0.86	e	0.042	0.118
K_t	12.2	10.5	A	0.3647	0.3647
$S_{p\,max}$	24.83	18.67	E	1128.45	1128.45
Q_{max}	38.32	5.85	T	297.15	297.15
Q_{min}	0.92	0.12	K_b	8.314	8.314
K_a	1.86	1.85	β	0.6	0.6
K_d	0.01	0.005	α	55	55

3.1.2. Results of short-term phosphate absorption experiments of K. mikimotoi under P_i-deplete condition

The changes of N, WP, Q_c, and S_p of *K. mikimotoi* at 20 °C and 24 °C under the condition of P_i-deplete with time are shown in Fig. 3. With the initial cell density 0.2×10^8 cells L^{-1}, N showed a trend of fluctuation during the experiment at the condition of 20 °C. It increased in the first 9 days, decreased in the next 6 days, and increased in the last 3 days. N at 24 °C decreased in the first 3 days, then increased in the latter 9 days and dropped again in the final 6 days. With the initial P_i concentration in substrate 0.74 μM, WP at 20 °C was almost the same as WP at 24 °C, ultimately reached a plateau after a sharp initial decline. With the initial Q_c 4.57×10^{-8} μmol $cell^{-1}$, Q_c decreased almost linearly in the course of the experiment at two temperatures. In the first 12 days, the trend of decline was relatively fast, and in the last 6 days reached a plateau. With the initial S_p 11.43×10^{-8} μmol $cell^{-1}$, S_p at 24 °C decreased soon after increasing in the first 3 days, while S_p at 20 °C decreased during the first 6 days, finally S_p tended to a plateau at both temperatures.

3.2. Experimental data fitting

The model calibration and validation results are shown in Figs. 4, 5, 6, and 7. Table 4 shows the model cost and relative error of all state

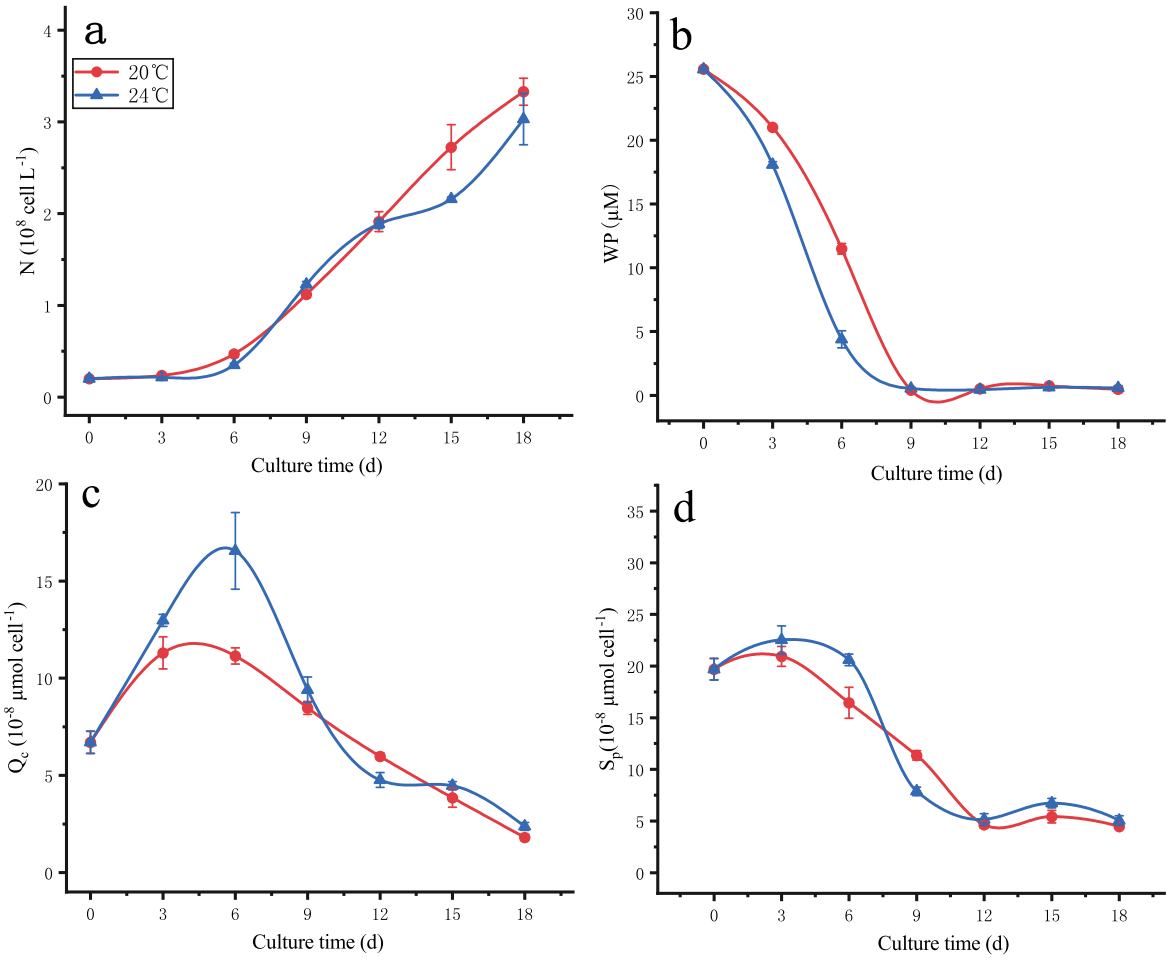

Fig. 2. Experimental results of P_i uptake of *K. mikimotoi* at 20 °C and 24 °C under the condition of P_i-replete. Here a–d are respectively the cell density (N), the concentration of P_i in the substrate (WP), the cell quota of QP (Q_c) and the cell quota of AP (S_p).

variables in model calibration and validation. The model fitting results of the experimental data of *K. mikimotoi* under P_i-replete condition at 24 °C are shown in Fig. 4. Among the four variables, Q_c has the best simulation effect, model cost and relative error both are the smallest, which are 0.63 and −2.79, respectively. The algal cell density N and the substrate P_i concentration WP are simulated moderately well with relative error of 11.21 and −13.83, respectively. For S_p, the simulated curve shows a trend similar to the observed curve and can better simulate the observation data of the first 9 days. However, the model cannot fit the observed data for the last 9 days, and simulation data is lower than the observation data. The fitting results of model (8) under the condition of P_i-deplete at 24 °C are given in Fig. 5. The simulation of Q_c performed the best with the model cost of 1.86 and the relative error of 15.34. For N and S_p, the model fitting curve and experimental data have similar trends, but can only fit some data points. For WP, the model can well fit the variation trend of experimental data, but in most cases, the observed value of WP is underestimated. The calibrated parameter values are displayed in Table 3. Figs. 6 and 7 show the model validation results of the experimental data of *K. mikimotoi* under the conditions of P_i-replete and P_i-deplete at 20 °C. It can be seen that the experimental data at 20 °C can be well fitted by using the trained model, here the model parameter values from in Table 3 and only change the temperature value. Combined with the calibration and validation results of model (8), it can be seen that the novel two-stage kinetics model can well describe the P_i uptake characteristics of algae at different P_i concentrations and temperatures.

4. Discussion

In the previous paper (Jiang et al., 2019), we focused on the comparison between the one-stage model and the two-stage model to study the P_i uptake kinetics by algae (*P. donghaiense*). In this study, the effects of different P_i concentrations and temperatures on the P_i uptake characteristics of *K. mikimotoi* are mainly considered. Combined with the experimental data and the fitting results of the model, it can be found that the P_i uptake characteristics of *K. mikimotoi* are different under different P_i concentrations and temperatures. Through these P_i uptake characteristics, the interspecific competition mechanism of two species *P. donghaiense* and *K. mikimotoi* during the red tide can be furthered to understand.

4.1. *The role of temperature on* P_i *uptake*

The influence of temperature on the P_i uptake process of algae can be divided into two aspects. On the one hand, temperature affects the activity of rate-limiting enzymes, which could limit the photosynthesis of light saturation and regulate the amount of inorganic phosphorus transported into cells (Von Caemmerer and Farquhar, 1981; Stitt, 1986). When considering the influence of temperature on the rate-limiting enzymes, it is important to consider the independent effect of temperature on the maximum growth rate μ_{max}, which is temperature-dependent and related to P_i uptake directly (Bordel et al., 2009; Goldman and Carpenter, 1974). On the other hand, temperature

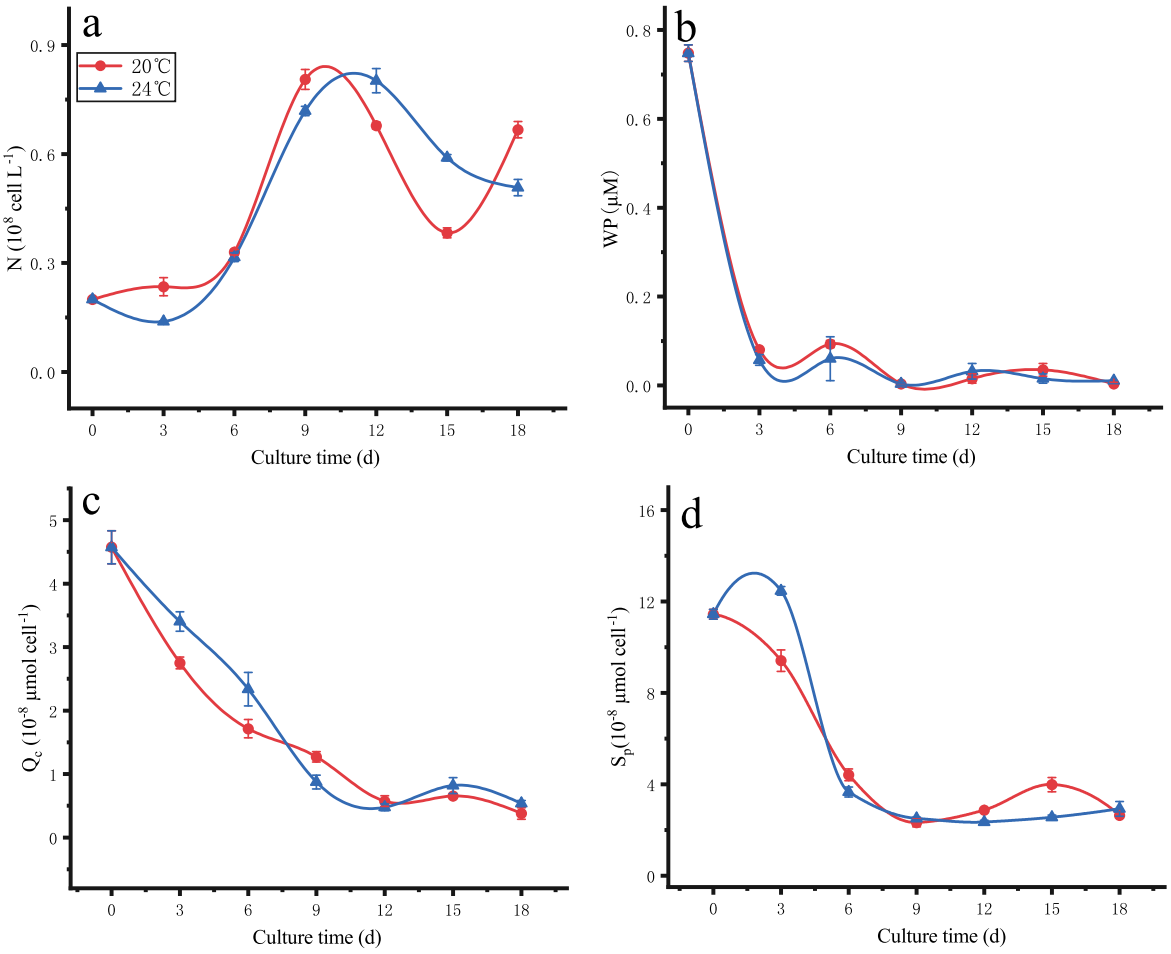

Fig. 3. Experimental results of P_i uptake of *K. mikimotoi* at 20 °C and 24 °C under the condition of P_i-deplete. Here panels a–d have the similar biological explanations as in Fig. 2.

Table 4
Model cost and relative error of all variables in model calibration and validation.

State variable	24 °C (P_i-replete)		24 °C (P_i-deplete)		20 °C (P_i-replete)		20 °C (P_i-deplete)	
	Cost	RE	Cost	RE	Cost	RE	Cost	RE
N	0.73	11.21	2.1	25.37	0.28	0.47	1.41	16.31
WP	4.79	−13.83	2.05	−43.27	6.34	−21.12	2.18	−44.92
Q_c	0.63	−2.79	1.86	15.34	0.2	10.66	1.45	15.22
S_p	2.60	−36.03	2.20	16.62	2.51	−35.65	2.66	18.10

could influence other enzymes and physical processes (Raven and Smith, 1978; Raven and Geider, 1988), which may also indirectly influence on phosphorus transport process. Under the same P_i concentration in the substrate, *K. mikimotoi* showed different growth characteristics at different temperatures (Figs. 2a and 3a). One possible reason is that temperature can directly regulate algae growth through light fluctuations and nutrient availability. It strongly affects the composition of cells, the absorption rate of nutrients, the fixation of carbon dioxide, and the growth rate of algae (Juneja et al., 2013; Ahmad et al., 2020). Furthermore, the peak values of Q_c and S_p at 24 °C were higher than those at 20 °C in both P_i-replete and P_i-deplete (see Figs. 2c, d, 3c, and d).

4.2. The role of P_i concentration on P_i uptake

Phosphorus is one of the main elements in phytoplankton growth, which is directly engaged in many processes of photosynthesis, such as the Calvin cycle and adjustment of some enzymes activity (Wang et al., 2004; Shen and Li, 2016). In the present study, *K. mikimotoi* obviously grows fast under P_i-replete than those under P_i-deplete (Figs. 2a and 3a). One possible reason for this phenomenon is that the growth rate of algae is proportional to the P_i concentration in a range of low and medium P_i concentrations (Long and Du, 2005; Shen and Li, 2016). About the condition of low P_i concentration, *K. mikimotoi* ended the exponential growth phase earlier and entered the decline phase (Figs. 2a and 3a). This may be due to the luxury uptake of P_i by algal cells under low phosphorus conditions, which increases the growth rate of cells in a short time, thus rapidly entering the exponential growth period to reach the peak, and then entering the decrease stage due to the depletion of phosphorus.

The decrease of Q_c of *K. mikimotoi* from day 6 to day 18 at 20 °C and 24 °C under the P_i-replete condition (Fig. 2c), which may be due to the dilution of intracellular P_i concentration caused by the increase of cell density (N), and the decrease of P_i concentration in the substrate (WP) resulted in the decrease of the amount of P_i transported into cells. The quantity Q_c decreased in *K. mikimotoi* during the whole treatment time at 20 °C and 24 °C under the condition of low P_i concentration (Fig. 3c). It may be because the P_i concentration of substrate was lower

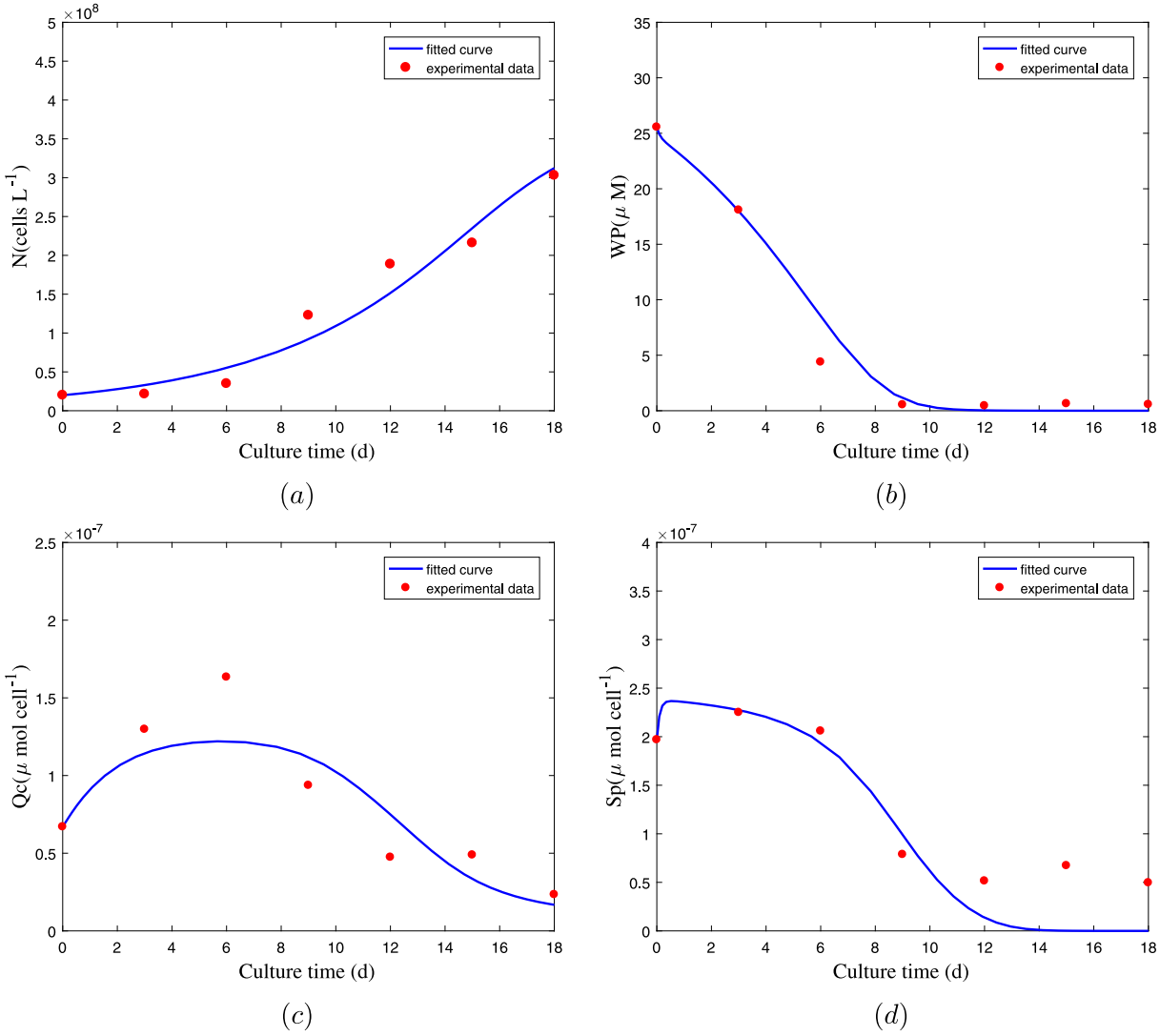

Fig. 4. Comparison of model fitted curve and experimental data of *K. mikimotoi* at 24 °C under the condition of P_i-replete. (a) N; (b) WP; (c) the cell quota of QP (Q_c); (d) the cell quota of AP (S_p). The parameters of model (8) can be estimated by fitting the four state variables at the same time. The parameter values are displayed in Table 3.

so that *K. mikimotoi* cannot grow and survive. Therefore, as cell density grew, previous cells had to allocate part of their own Q_c to newborn cells.

S_p reached its maximum value faster and entered into stable phase earlier under P_i-deplete than that at P_i-replete (Figs. 2d and 3d). The reason for this phenomenon may be that algal cells at the condition of low P_i concentration took little time to make P_i of surface-adsorbed transfer into intracellular than that at high P_i concentration. Furthermore, this can be explained as dinoflagellate cells can accelerate P_i uptake by increasing the number of high affinity phosphate transporters when the deterioration of the external environment is in the state of phosphorus stress (Lin et al., 2016). In model (8), a decreasing function K_p of external phosphorus concentration is used to describe this phenomenon. When P_i is deficient, K_p has a large value, and the uptake rate of P_i by algal cells increased at this time. In addition, the parameter values of $Q_{\max}$, $Q_{\min}$, and $S_{p\max}$ at P_i-replete group were higher than those at P_i-deplete group (Table 3). This may be because when phosphorus is sufficient, the survival strategy of algae cell has changed, increasing its internal and external P_i pools and storing a large amount of P_i to cope with sudden deterioration of the external environment (Kwon et al., 2013). The value of e at P_i-replete is lower than that at P_i-deplete, which may be increased cell mortality due to the lack of nutrition in the environment.

Table 5
Indices of P_i uptake characteristics of *K. mikimotoi* and *P. donghaiense* at 24 °C under different P_i concentrations.

Indices of P_i uptake kinetics	*K. mikimotoi*		*P. donghaiense*	
	P_i-replete	P_i-deplete	P_i-replete	P_i-deplete
R(unitless)	41.65	48.75	26.87	26.87
T_g(day)	16.45	16.83	8.76	8.45

4.3. The role of P_i uptake on the competition between *K. mikimotoi* and *P. donghaiense*

Jiang et al. (2019) studied the P_i uptake characteristics of *P. donghaiense* by using the two-stage kinetics model under different P_i concentrations, compared it with the one-stage kinetics model, and found that the two-stage kinetics process was better than one stage kinetics process. Here the mechanism of competition between *P. donghaiense* and *K. mikimotoi* under various P_i concentrations at 24 °C will be discussed.

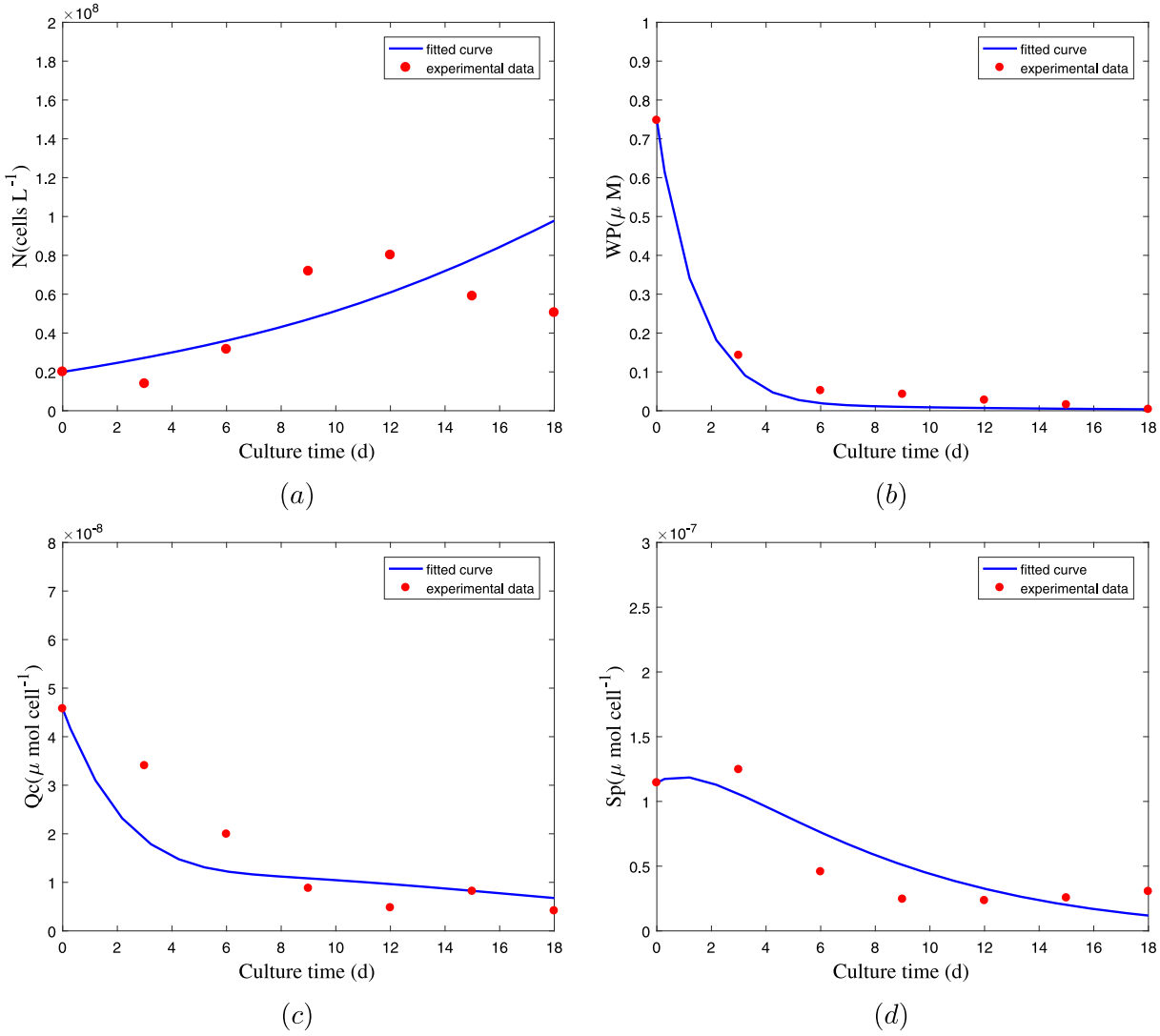

Fig. 5. Comparison of model fitted curve and experimental data of *K. mikimotoi* at 24 °C under the condition of P_i-deplete. (a) N; (b) WP; (c) the cell quota of QP (Q_c); (d) the cell quota of AP (S_p). The parameters of model (8) can be estimated by fitting the four state variables at the same time. The parameter values are displayed in Table 3.

Droop first proposed the concept of luxury coefficient R ($Q_{\max}/Q_{\min}$) and used it to express the nutritional storage capacity of algal cells. A larger R gives a stronger P_i storage capacity of algal cells (Droop, 1974; Li, 2007). The utility value of the nutrient storage in algal cells for cell growth depends also on the maximum growth rate of the algae. For this reason, Pedersen and Borum (1996) proposed the concept of growth potential T_g ($\ln R/\mu_{\max}$) to evaluate the utility of nutrients stored in algal cells for cell growth and reproduction. Table 5 shows the calculation results of luxury coefficient R and growth potential T_g of *K. mikimotoi* and *P. donghaiense* at two P_i concentrations of 24 °C. The values of R of *P. donghaiense* and *K. mikimotoi* under P_i-replete condition at 24 °C are 26.87 (Jiang et al., 2019) and 41.68, respectively. T_g values of *P. donghaiense* and *K. mikimotoi* under P_i-replete condition at 24 °C are 8.76 (Jiang et al., 2019) and 16.45, respectively. The higher values of R and T_g of *K. mikimotoi* than those of *P. donghaiense* under the condition of P_i-replete concentration at 24 °C imply that the viability of *K. mikimotoi* is better than *P. donghaiense* in the bi-algae substrate at higher temperature under P_i-replete condition (24 °C and 28 °C) (Shen et al., 2014). Similarly, the large values of R and T_g in *K. mikimotoi* (48.75, 16.83) than those in *P. donghaiense* (26.84, 8.45) under P_i-deplete condition at 24 °C imply that the viability of *K. mikimotoi* is also better than *P. donghaiense* in bi-algal culture medium under P_i-deplete condition at 24 °C.

5. Conclusion

Based on the two-stage model in our previous work (Jiang et al., 2019), a novel two-stage kinetics model is developed by combining the Arrhenius temperature function and P_i stress function. This model will help predict P_i uptake kinetics of algae at different phosphorus and temperatures concentrations. The model parameters are calibrated by the experimental data of *K. mikimotoi* at 24 °C under the conditions of P_i-replete and P_i-deplete, and then the model is validated by the experimental data of two P_i concentrations at 20 °C. Experimental data and fitting results suggest that the P_i uptake characteristics of the *K. mikimotoi* vary under different cultural conditions of P_i concentration and temperature. Furthermore, by using the results of experiments and parameter values, the interspecific competition between two species *K. mikimotoi* and *P. donghaiense* under different P_i concentrations are discussed. In order to predict the occurrence of algal blooms in oceans using observational information from marine and experimental results, some factors need to be explored further, for example, pH value, solar irradiance, water velocity, environmental toxins and the direct or indirect interactions of algal species (Yang and Yuan, 2021; Xu et al., 2021). Constraints of solar irradiance and phosphate on algae or algae-*Daphnia* interactions were modeled in Wang et al. (2008), Li and Wang (2012), Peace et al. (2014), Peace and Wang (2019), Yuan et al. (2020),

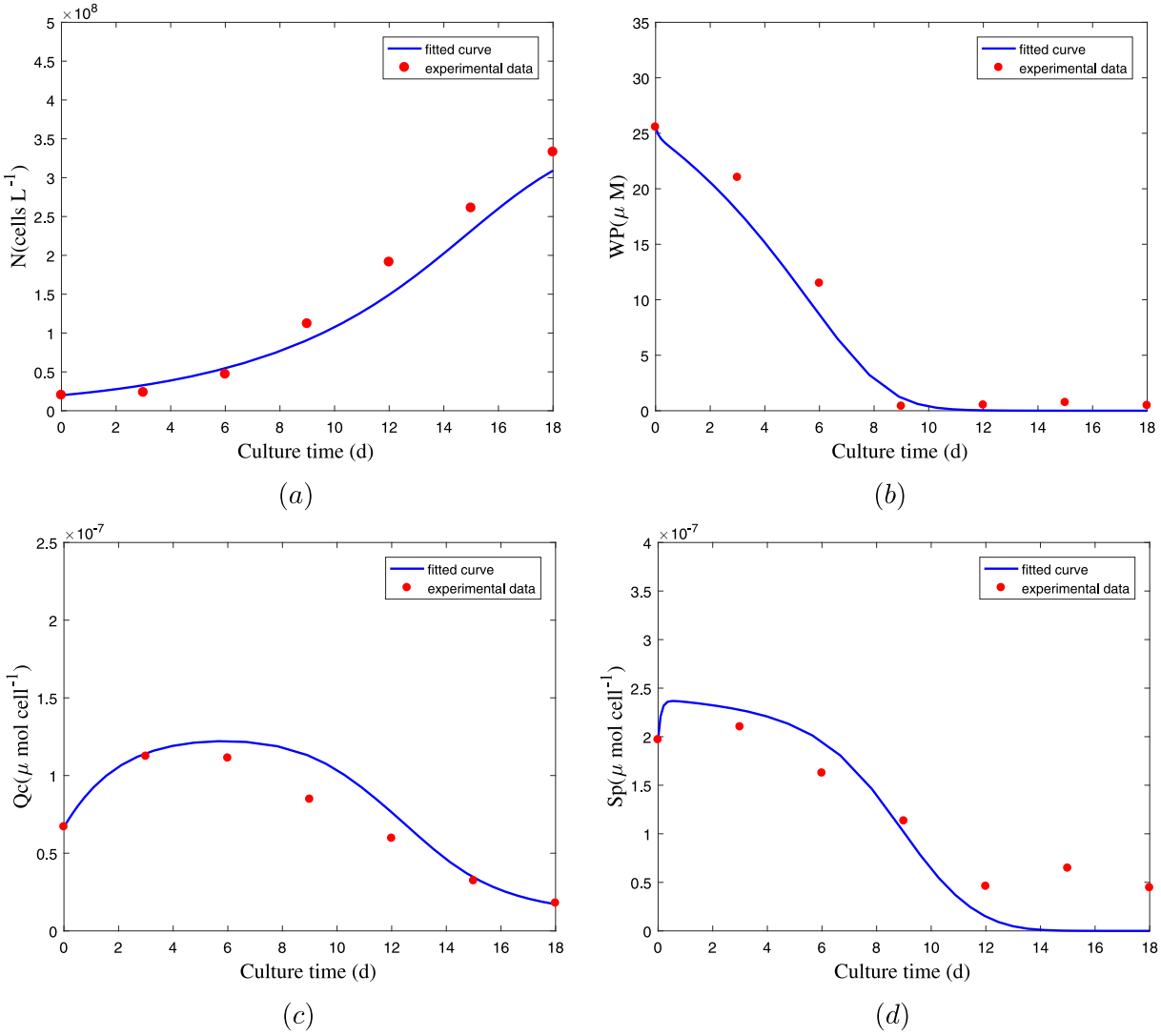

Fig. 6. Validation of model (8) with the data of four state variables of *K. mikimotoi* under the condition of P_i-replete at 20 °C. Here $T = 293.15$ and the rest parameter values are from in Table 3.

Davies and Wang (2021) and Zhao et al. (2020) via stoichiometric theory. The integration of stoichiometric models with the multi-stage algal nutrient uptake process would provide a fundamental modeling framework of nutrient cycling and energy flow in trophic cascades. This would be a promising cutting-edge area to explore in the future.

CRediT authorship contribution statement

Shufei Gao: Conducted and analysis data, Writing – original draft. **Anglu Shen:** Conducted the experimental work, Conducted and analysis data, Writing – original draft. **Jie Jiang:** Conducted and analysis data, Writing – original draft. **Hao Wang:** Designed this study, Commented and amended on the manuscript. **Sanling Yuan:** Designed this study, Commented and amended on the manuscript.

Declaration of competing interest

The authors declare that they have no known competing financial interests or personal relationships that could have appeared to influence the work reported in this paper.

Data accessibility

All data used in this study can be found in the manuscript and its supplementary materials.

Acknowledgments

We are very grateful to both the editor and the reviewers for their valuable comments and suggestions, which have greatly improved the quality and presentation of our paper. The research was funded by the National Natural Science Foundation of China (grant numbers 11671260, 12071293, 41506194). This work was also funded by the Special Fund for National Non-profit Institutes (grant number 2015M06) and the Natural Sciences and Engineering Research Council of Canada (grant numbers RGPIN-2020-03911, RGPAS-2020-00090).

Appendix A. Supplementary data

Supplementary material related to this article can be found online at https://doi.org/10.1016/j.ecolmodel.2022.109909.

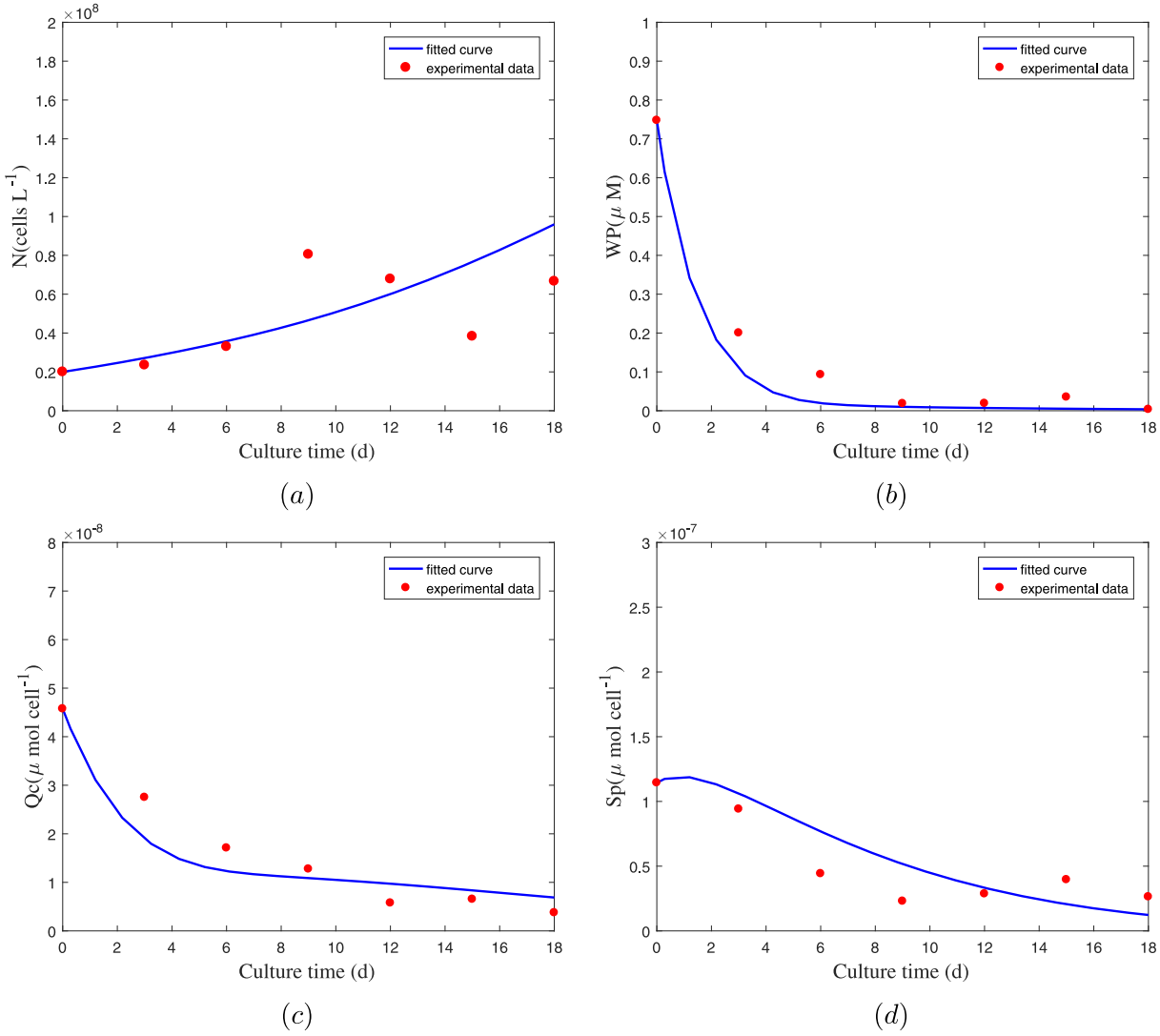

Fig. 7. Validation of model (8) with the data of four state variables of *K. mikimotoi* under the condition of P_i-deplete at 20 °C. Here $T = 293.15$ and the rest parameter values are from in Table 3.

References

Adhurya, S., Das, S., Ray, S., 2021. Simulating the effects of aquatic avifauna on the Phosphorus dynamics of aquatic systems. Ecol. Model. 445, 109495. http://dx.doi.org/10.1016/j.ecolmodel.2021.109495.

Ahmad, S., Kothari, R., Shankarayan, R., Tyagi, V.V., 2020. Temperature dependent morphological changes on algal growth and cell surface with dairy industry wastewater: an experimental investigation. 3 Biotech. 10 (1), 1–12. http://dx.doi.org/10.1007/s13205-019-2008-x.

Aksnes, D.L., Egge, J.K., 1991. A theoretical model for nutrient uptake in phytoplankton. Mar. Ecol. Prog. Ser. 70 (1), 65–72. http://dx.doi.org/10.3354/meps070065.

Bordel, S., Guieysse, B., Munoz, R., 2009. Mechanistic model for the reclamation of industrial wastewaters using algal-bacterial photobioreactors. Environ. Sci. Technol. 43 (9), 3200–3207. http://dx.doi.org/10.1021/es802156e.

Brand, L.E., Campbell, L., Bresnan, E., 2012. Karenia: The biology and ecology of a toxic genus. Harmful Algae 14 (Feb.), 156–178. http://dx.doi.org/10.1016/j.hal.2011.10.020.

Chang, F.H., 2011. Toxic effects of three closely-related dinoflagellates, *Karenia concordia*, *K. brevisulcata* and *K. mikimotoi* (Gymnodiniales, dinophyceae) on other microalgal species. Harmful Algae 10 (2), 181–187. http://dx.doi.org/10.1016/j.hal.2010.09.004.

Chen, C.S., Zhu, J.R., Beardsley, R.C., Franks, P.J.S., 2003. Physical-biological sources for dense algal blooms near the Changjiang River. Geophys. Res. Lett. 30 (10), 405–414. http://dx.doi.org/10.1029/2002GL016391.

Davies, C.M., Wang, H., 2021. Contrasting stoichiometric dynamics in terrestrial and aquatic grazer–producer systems. J. Biol. Dyn. 15 (sup1), S3–S34. http://dx.doi.org/10.1080/17513758.2020.1771442.

Davison, I.R., 1991. Environmental effects on algal photosynthesis: temperature. J. Phycol. 27 (1), 2–8. http://dx.doi.org/10.1111/j0022-3646.1991.00002.x.

Droop, M.R., 1973. Some thoughts on nutrient limitation in algae. J. Phycol. 9 (3), 264–272. http://dx.doi.org/10.1111/j.1529-8817.1973.tb04092.x.

Droop, M.R., 1974. The nutrient status of algal cells in continuous culture. J. Mar. Biol. Assoc. U.K. 54 (4), 825–855. http://dx.doi.org/10.1017/s002531540005760x.

Droop, M.R., 1983. 25 Years of Algal Growth Kinetics a Personal View. Walter de Gruyter, Berlin/New York Berlin, New York, http://dx.doi.org/10.1515/botm.1983.26.3.99.

Dyhrman, S.T., Palenik, B., 1999. Phosphate stress in cultures and field populations of the dinoflagellate *Prorocentrum minimum* detected by a single-cell alkaline phosphatase assay. Appl. Environ. Microbiol. 65 (7), 3205–3212. http://dx.doi.org/10.1053/jvet.2003.50040.

Goldman, J.C., Carpenter, E.J., 1974. A kinetic approach to the effect of temperature on algal growth. Limnol. Oceanogr. 19 (5), 756–766. http://dx.doi.org/10.4319/lo.1974.19.5.0756.

Goldman, J.C., Taylor, C.D., Glibert, P.M., 1981. Nonlinear time-course uptake of carbon and ammonium by marine phytoplankton. Mar. Ecol. Prog. 6 (2), 137–148. http://dx.doi.org/10.3354/meps006137.

Guillard, R.R.L., 1975. Culture of phytoplankton for feeding marine invertebrates. In: Culture of Marine Invertebrate Animals. Springer, pp. 29–60.

Harrison, P.J., Conway, H.L., Davis, C.O., 1976. Marine diatoms grown in chemostats under silicate or ammonium limitation. II. Transient response of *Skeletonema costatum* to a single addition of the limiting nutrient. Mar. Biol. 35 (2), http://dx.doi.org/10.1007/BF00390940.

Harrison, P.J., Parslow, J.S., Conway, H.L., 1989. Determination of nutrient uptake kinetic parameters: a comparison of methods. Mar. Ecol. Prog. Ser. 301–312. http://dx.doi.org/10.3354/meps052301.

Helbling, E.W., Buma, A.G., Boelen, P., Van der Strate, H.J., Giordanino, M.V.F., Villafañe, V.E., 2011. Increase in rubisco activity and gene expression due to elevated temperature partially counteracts ultraviolet radiation–induced photoinhibition in the marine diatom *Thalassiosira weissflogii*. Limno. Oceanogr. 56 (4), 1330–1342. http://dx.doi.org/10.4319/lo.2011.56.4.1330.

Jiang, J., Shen, A.L., Wang, H., Yuan, S.L., 2019. Regulation of phosphate uptake kinetics in the bloom-forming dinoflagellates *prorocentrum donghaiense* with emphasis on two-stage dynamic process. J. Theoret. Biol. 463, 12–21. http://dx.doi.org/10.1016/j.jtbi.2018.12.011.

Jin, J., Liu, S., Ren, J., 2021. Phosphorus utilization by phytoplankton in the yellow sea during spring bloom: Cell surface adsorption and intracellular accumulation. Mar. Chem. 231 (3), 103935. http://dx.doi.org/10.1016/j.marchem.2021.103935.

John, E.H., Flynn, K.J., 2000. Modelling phosphate transport and assimilation in microalgae; how much complexity is warranted? Ecol. Model. 125 (2–3), 145–157. http://dx.doi.org/10.1016/S0304-3800(99)00178-7.

Juneja, A., Ceballos, R., Murthy, G., 2013. Effects of environmental factors and nutrient availability on the biochemical composition of algae for biofuels production: A review. Energies 6 (9), 4607–4638. http://dx.doi.org/10.3390/en6094607.

Karentz, D., Smayda, T.J., 1984. Temperature and seasonal occurrence patterns of 30 dominant phytoplankton species in Narragansett Bay over a 22-year period (1959–1980). Mar. Ecol. Prog. Ser. 277–293. http://dx.doi.org/10.1007/BF02790626.

Kwon, H.K., Oh, S.J., Yang, H.-S., 2013. Growth and uptake kinetics of nitrate and phosphate by benthic microalgae for phytoremediation of eutrophic coastal sediments. Bioresour. Technol. 129, 387–395. http://dx.doi.org/10.1016/j.biortech.2012.11.078.

Lee, E., Jalalizadeh, M., Zhang, Q., 2015. Growth kinetic models for microalgae cultivation: a review. Algal Res. 12, 497–512. http://dx.doi.org/10.1016/j.algal.2015.10.004.

Lehman, J.T., Sandgren, C.D., 1982. Phosphorus dynamics of the procaryotic nannoplankton in a Michigan lake. Limnol. Oceanogr. 27 (5), 828–838. http://dx.doi.org/10.4319/lo.1982.27.5.0828.

Li, Z.F., 2007. The eco-physiological studies of phosphorus on the growth of *Karenia mikimotoi* Hansen. Jinan Univ. 1–47.

Li, J., Glibert, P.M., Zhou, M.J., Lu, S.H., Lu, D.D., 2009. Relationships between nitrogen and phosphorus forms and ratios and the development of dinoflagellate blooms in the East China Sea. Mar. Ecol. Prog. 383 (may 14), 11–26. http://dx.doi.org/10.3354/meps07975.

Li, X., Wang, H., 2012. A stoichiometrically derived algal growth model and its global analysis. Math. Biosci. Eng. 7 (4), 825–836. http://dx.doi.org/10.3934/mbe.2010.7.825.

Li, X.D., Yan, T., Yu, R.C., Zhou, M.J., 2019. A review of karenia mikimotoi: Bloom events, physiology, toxicity and toxic mechanism. Harmful Algae 90, 101702. http://dx.doi.org/10.1016/j.hal.2019.101702.

Lin, S.J., Litaker, R.W., Sunda, W.G., 2016. Phosphorus physiological ecology and molecular mechanisms in marine phytoplankton. J. Phycol. 52 (1), 10–36. http://dx.doi.org/10.1111/jpy.12365.

Liu, X.A., Ran, Y., Luo, Y.F., 2007. Multi-layer model for algal growth under different behaviors of nutritious salt. Environ. Sci. 28 (10), 2163–2168. http://dx.doi.org/10.13227/j.hjkx.2007.10.004.

Long, H., Du, Q., 2005. Primary research on karenia mikimotoi bloom in Fujian coast. J. Fujian Fish. 4, 22–26. http://dx.doi.org/10.3969/j.issn.1006-5601.2005.04.006.

Lü, S.H., Cen, J.Y., Wang, J.Y., Ou, L.J., 2019. The research status quo, hazard, and ecological mechanisms of *Karenia mikimotoi* red tide in coastal waters of China. Oceanol. Limnol. Sinica 50, 487–494.

Marois, D.E., Mitsch, W.J., 2016. Modeling phosphorus retention at low concentrations in Florida Everglades mesocosms. Ecol. Model. 319, 42–62. http://dx.doi.org/10.1016/j.ecolmodel.2015.09.024.

Morel, F.M.M., 1987. Kinetics of nutrient uptake and growth in phytoplankton. J. Phycol. 23 (1), 137–150. http://dx.doi.org/10.1016/0198-0254(87)90278-0.

Ou, L.J., Wang, D., Huang, B.Q., Hong, H.S., Qi, Y.Z., Lu, S.H., 2008. Comparative study of phosphorus strategies of three typical harmful algae in Chinese coastal waters. J. Plankton Res. 30 (9), 1007–1017. http://dx.doi.org/10.1093/plankt/fbn058.

Peace, A., Wang, H., 2019. Compensatory foraging in stoichiometric producer–grazer models. Bull. Math. Biol. 81 (12), 4932–4950. http://dx.doi.org/10.1007/s11538-019-00665-2.

Peace, A., Wang, H., Kuang, Y., 2014. Dynamics of a producer–grazer model incorporating the effects of excess food nutrient content on grazer's growth. Bull. Math. Biol. 76 (9), 2175–2197. http://dx.doi.org/10.1007/s11538-014-0006-z.

Pedersen, M., Borum, J., 1996. Pedersennutrient control of algal growth in estuarine waters. Nutrient limitation and the importance of nitrogen requirements and nitrogen storage among phytoplankton and species of macroalgae. Mar. Ecol. Prog. Ser. 142 (1–3), 261–272. http://dx.doi.org/10.3354/meps142261.

Raven, J.A., Geider, R.J., 1988. Temperature and algal growth. New Phytol. 110 (4), 441–461. http://dx.doi.org/10.1111/j.1469-8137.1988.tb00282.x.

Raven, J.A., Smith, F.A., 1978. Effect of temperature and external pH on the cytoplasmic pH of Chara corallina. J. Exp. Bot. 29 (4), 853–866. http://dx.doi.org/10.1093/jxb/29.4.853.

Rengefors, K., Ruttenberg, K., Haupert, C., Taylor, C., Howes, B., Anderson, D., 2003. Experimental investigation of taxon-specific response of alkaline phosphatase activity in natural freshwater phytoplankton. Limnol. Oceanogr. 48 (3), 1167–1175. http://dx.doi.org/10.4319/lo.2003.48.3.1167.

Riegman, R., Mur, L.R., 1984. Regulation of phosphate uptake kinetics in Oscillatoria agardhii. Arch. Microbiol. 139 (1), 28–32. http://dx.doi.org/10.1007/bf00692707.

Sañudo-Wilhelmy, S., Tovar-Sanchez, A., Fu, F.X., Capone, D.G., Carpenter, E.J., Hutchins, D.A., 2004. The impact of surface-adsorbed phosphorus on phytoplankton Redfield stoichiometry. Nature 432 (7019), 897–901. http://dx.doi.org/10.1038/nature03125.

Shen, A.L., Li, D.J., 2016. Effects of different nutrients levels on the growth of *Procentrum donghaiense* and *Karenia mikimotoi*. Mar. Fish. 38 (4), 416–422. http://dx.doi.org/10.13233/j.cnki.mar.fish.2016.04.009.

Shen, A.L., Ma, Z.L., Jiang, K.J., Li, D.J., 2016. Effects of temperature on growth, photophysiology, Rubisco gene expression in *Prorocentrum donghaiense* and *Karenia mikimotoi*. Ocean Sci. J. 51 (4), 581–589. http://dx.doi.org/10.1007/s12601-016-0056-2.

Shen, A.L., Yuan, X.W., Liu, G.P., Li, D.J., 2014. Growth interactions between the bloom-forming dinoagellates *Prorocentrum donghaiense* and *Karenia mikimotoi* under different temperature. Thalassas 30, 33–45.

Singh, D., Nedbal, L., Ebenhöh, O., 2018. Modelling phosphorus uptake in microalgae. Biochem. Soc. T. 46 (2), 483–490. http://dx.doi.org/10.1042/BST20170262.

Stitt, M., 1986. Limitation of photosynthesis by carbon metabolism: I. Evidence for excess electron transport capacity in leaves carrying out photosynthesis in saturating light and CO2. Plant Physiol. 81 (4), 1115–1122. http://dx.doi.org/10.1104/pp.81.4.1115.

Uchida, T., Toda, S., Matsuyama, Y., Yamaguchi, M., Kotani, Y., Honjo, T., 1999. Interactions between the red tide dinoflagellates *Heterocapsa circularisquama* and *Gymnodinium mikimotoi* in laboratory culture. J. Exp. Mar. Biol. Ecol. 241 (2), 285–299. http://dx.doi.org/10.1016/S0022-0981(99)00088-X.

Von Caemmerer, S., Farquhar, G.D., 1981. Some relationships between the biochemistry of photosynthesis and the gas exchange of leaves. Planta 153 (4), 376–387. http://dx.doi.org/10.2307/23375285.

Wang, X.L., Deng, N.N., Zhu, C.J., Han, X.R., Li, K.Q., Xin, Y., Chen, L.L., 2004. Effect of nutrients (phosphate and nitrate) composition on the growth of HAB algae. J. Ocean Univ. China 3, http://dx.doi.org/10.16441/j.cnki.hdxb.2004.03.016.

Wang, H., Kuang, Y., Loladze, I., 2008. Dynamics of a mechanistically derived stoichiometric producer-grazer model. J. Biol. Dyn. 2 (3), 286–296. http://dx.doi.org/10.1080/17513750701769881.

Xu, C.Q., Yuan, S.L., Zhang, T.H., 2021. Competitive exclusion in a general multi-species chemostat model with stochastic perturbations. Bull. Math. Biol. 83 (1), 1–17. http://dx.doi.org/10.1007/s11538-020-00843-7.

Yang, J.G., Yuan, S.L., 2021. Dynamics of a toxic producing phytoplankton-zooplankton model with three-dimensional patch. Appl. Math. Lett. 118 (3), http://dx.doi.org/10.1016/j.aml.2021.107146.

Yao, B., Xi, B.D., Hu, C.M., Huo, S.L., Su, J., Liu, H.L., 2011. A model and experimental study of phosphate uptake kinetics in algae: considering surface adsorption and P-stress. J. Environ. Sci. 23 (2), 189–198. http://dx.doi.org/10.1016/S1001-0742(10)60392-0.

Yuan, S.L., Wu, D.M., Lan, G.J., Wang, H., 2020. Noise-induced transitions in a nonsmooth Producer–Grazer model with stoichiometric constraints. Bull. Math. Biol. 82 (5), 1–22. http://dx.doi.org/10.1007/s11538-020-00733-y.

Zhao, D.Z., 2010. Occurrence Regularity of Marine Red Tide Disaster in Typical Areas in China. Marine Press, Beijing, p. 44.

Zhao, S.N., Yuan, S.L., Wang, H., 2020. Threshold behavior in a stochastic algal growth model with stoichiometric constraints and seasonal variation. J. Differential Equations 268 (9), 5113–5139. http://dx.doi.org/10.1016/j.jde.2019.11.004.

Zhou, Z.X., Yu, R.C., Zhou, M.J., 2017a. Resolving the complex relationship between harmful algal blooms and environmental factors in the coastal waters adjacent to the Changjiang River estuary. Harmful Algae 62, 60. http://dx.doi.org/10.1016/j.hal.2016.12.006.

Zhou, Z.X., Yu, R.C., Zhou, M.J., 2017b. Seasonal succession of microalgal blooms from diatoms to dinoflagellates in the East China Sea: A numerical simulation study. Ecol. Model. 360, 150–162. http://dx.doi.org/10.1016/j.ecolmodel.2017.06.027.